

Determination of Structure and Energetics for Gibbs Surface Adsorption Layers of Binary Liquid Mixture 2. Methanol + Water

Hua Chen,[†] Wei Gan,[†] Rong Lu,^{†,‡} Yuan Guo, and Hong-fei Wang*

State Key Laboratory of Molecular Reaction Dynamics, Institute of Chemistry, Chinese Academy of Sciences, Beijing, P.R. China 100080

Received: January 11, 2005; In Final Form: February 27, 2005

Vapor/methanol and vapor/methanol–water mixture interfaces have been among the benchmark liquid interfaces under extensive experimental and theoretical investigation. In this report, we studied the orientation, structure and energetics of the vapor/methanol–water interface with newly developed techniques in sum frequency generation vibrational spectroscopy (SFG-VS). Different from the interpretations in previous SFG-VS studies for a more disordered interface at higher bulk methanol concentrations, we found that the methanol–water mixture interface is well ordered in the whole concentration region. We are able to do so because direct polarization null angle (PNA) measurement allowed us to accurately determine the CH₃ orientation at the interface and to separate the orientational and interface density contributions to the SFG-VS signal. We found that the CH₃ groups at the interface pointed out almost perpendicularly from the interface. We further found that this well-ordered vapor/methanol–water mixture interface has an antiparallel structure. With the double layer adsorption model (DAM) and Langmuir isotherm, the adsorption free energies for the first and second layer are obtained as -1.7 ± 0.1 kcal/mol and 0.5 ± 0.4 kcal/mol, respectively. Therefore, the second layer adsorption is slightly negative, and this means that replacement of the second layer water molecule with methanol molecule is energetically unfavorable. Comparing this interface with the vapor/acetone–water mixture interface reported previously, we are able to correlate the second layer adsorption free energy with the work of self-association using the pairwise self- and mutual interaction energies between the water and solute molecules. These results provided detailed microscopic structural evidences for understanding of liquid interfaces.

1. Introduction

This report is the second in the series of our studies on structure and energetics for Gibbs surface adsorption layers of binary liquid mixtures. In the preceding report we presented a detailed study on the vapor/acetone–water mixture interface at ambient temperature with sum frequency generation vibrational spectroscopy (SFG-VS).¹ The orientation of the interfacial acetone molecule is accurately determined with the polarization null angle (PNA) method in SFG-VS. The interfacial acetone molecule has its C=O group point into the bulk phase, one CH₃ group points up from the bulk, and the other CH₃ group points into the bulk phase. An antiparallel double layer adsorption structure was identified for the acetone–water mixture interface and, with the double layer adsorption model (DAM) and Langmuir isotherm, the adsorption free energies for the first and second layer are obtained as -1.9 ± 0.2 kcal/mol and -0.9 ± 0.2 kcal/mol, respectively. These results were consistent with previous MD simulations for the vapor/pure acetone interface and provided direct microscopic structural evidence and new insight for the understanding of liquid and liquid mixture interfaces. Most importantly, the experimental techniques and quantitative analysis methodology used for detailed measure-

ment of the acetone–water mixture interfaces can be applied to detailed understanding of other liquid interfaces, as well as other molecular interfaces in general.

In this report we shall present the SFG-VS study on the vapor/methanol–water mixture interface with the same approach. Vapor/methanol and vapor/methanol–water mixture interfaces have been among the benchmark liquid interfaces under extensive experimental and theoretical investigations. We shall demonstrate that the vapor/methanol–water mixture interface also forms an antiparallel double layer adsorption structure. The DAM and Langmuir isotherm are used to determine that the adsorption free energies for methanol–water mixture interface for the first and second layers are -1.7 ± 0.1 kcal/mol and 0.5 ± 0.4 kcal/mol, respectively. The most striking discoveries for us are not only the fact that the vapor/methanol–water mixture interface becomes more ordered with increasing bulk methanol concentration, different from the previous SFG-VS studies on the vapor/pure methanol and vapor/methanol–water mixture interfaces, but also the fact that the second layer adsorption exhibit a slightly negative adsorption isotherm with a small positive adsorption free energy.

Methanol is one of the most important liquid chemicals in chemical industry and is used primarily as fuel. It also has important environmental and biological importance. As the simplest alcohol, it is also a benchmark molecule for experimental and theoretical studies on thermodynamics, structure, and dynamics with hydrogen bonding in the bulk liquid or liquid mixtures,^{2–5} as well as for studies on liquid and liquid mixture interfaces.^{6–29} Even though the vapor/methanol and vapor/

* To whom correspondence should be addressed. E-mail: hongfei@mrdlab.icas.ac.cn. Tel. 86-10-62555347; Fax 86-10-62563167.

[†] Also graduate students of the Graduate school of the Chinese Academy of Sciences.

[‡] Currently at the Reaction and Excitation Dynamics Group, Materials Engineering Laboratory, National Institute for Material Science, Sengen, Tsukuba, Japan.

methanol–water mixture interfaces have been extensively studied, there are still disagreements between different studies.

One of the general issues for liquid and liquid mixture interface studies is the orientation or orientational order of the interfacial molecules. It has been commonly accepted that the surfaces of strongly hydrogen bonded liquids, such as water and methanol, are ordered.^{30,31} On this ground the problem is how well the order and how to accurately determine this interface order. Both SFG-VS experimental measurement and molecular dynamics (MD) simulations have provided such information to some extent.

The vapor/methanol interface is the first neat liquid studied with SFG-VS.⁶ SFG-VS and MD simulations have confirmed that the ordered CH₃ group of the interface methanol molecule points away from the liquid and liquid mixture interface.^{6–10,17–20,22,23,26,27,29} The ability to obtain relatively strong SFG-VS spectral peaks for the CH₃ groups at vapor/ethanol and vapor/methanol–water mixture interfaces indicates that the CH₃ groups are oriented at the interface. Previously reported SFG-VS experimental results concluded that the CH₃ groups at the vapor/pure methanol interface have a broad orientational distribution and the measurement with SFG-VS spectra at different polarization combinations indicated that the orientational angle, though it cannot be uniquely determined, was somewhere between the two extreme cases: one is $\theta = 40^\circ$ with the distribution width $\Delta\theta = 0^\circ$, and the other is $\theta = 0^\circ$ with $\Delta\theta = 110^\circ$, with θ as the orientational angle of the symmetry axis of the CH₃ group from the interface normal.^{6–10} Previously reported SFG-VS studies also agreed on the conclusion that at the aqueous mixture interface the CH₃ groups of methanol molecules are less ordered at higher bulk methanol concentration.^{7,8,10} These results are generally in accordance with the existing MD simulation studies on vapor/methanol and methanol–water mixture interfaces qualitatively.^{17–20,22,23,25–27,29}

Another general issue in liquid and liquid mixture interface studies is the roughness or the width of the interface. A few X-ray reflectivity measurements and MD simulations have provided such information. X-ray reflectivity measurement along with surface capillary wave (CW) theory by Pershan et al. gave the intrinsic roughness of the vapor/pure methanol interface as $\sigma_p = 0.7 \pm 0.4 \text{ \AA}$ and a capillary wave roughness $\sigma_c \sim 4.65$ to 4.85 \AA .¹³ These results further indicated that the vapor/methanol interface is somewhat oriented because σ_p measured is less than the mean radius of the methanol molecule.¹³ These results are in agreement with the MD simulation results, which ended up with calculated thickness from the interface density and energy profiles for the vapor/methanol and vapor/methanol–water mixture interfaces ranging from 2.0 \AA to 4.6 \AA (if using the 10–90 definition of thickness, the numbers should be around 8 \AA).^{17–20,22,23,25–27,29} These results clearly indicated that the interfacial region is about one or two molecular layers thick. A recent surface sensitive extended X-ray absorption fine structure (EXAFS) study of the liquid methanol jet surface by Saykally et al.¹⁴ suggested that the vapor/methanol interface has a strongly oriented outermost layer and a “hydrophobic packing” structure. This double layer structure for the vapor/methanol interface is similar to that for the vapor/acetone interface.^{1,32} This picture also suggested a relatively narrow orientational distribution of the CH₃ groups at the vapor/methanol interface. It is, therefore, not in full agreement with the previous SFG-VS studies.

Since the previous SFG-VS measurements of orientation of interfacial molecular groups had allowed too much room for speculation, we have been trying to develop a novel method for more accurate orientation measurement with SFG-VS.^{11,33}

A recent measurement on the molecular orientation at the vapor/methanol interface in our laboratory gave a surprising result. Using the newly developed PNA method³³ in SFG-VS,¹¹ we accurately determined the orientational angle of the CH₃ groups at the vapor/methanol interface at room temperature and we concluded that $\theta = 0^\circ \pm 6^\circ$ with a very narrow orientational distribution.¹¹ In this study the orientational parameter $D = \langle \cos\theta \rangle / \langle \cos^3\theta \rangle$ for the interfacial CH₃ groups of the methanol molecules is accurately determined as $D = 0.97 \pm 0.04$. As was demonstrated previously, if there is only one kind of CH₃ group at the interface, both the δ -distribution function and a broad Gaussian distribution function for θ would simply make $D \geq 1$.^{33–36} $D \equiv 1$ is only possible when the tilt angle $\theta = 0^\circ$ and the distribution width $\Delta\theta = 0^\circ$, and any D value very close to 1 means that the interfacial groups are well ordered and stand straight at the interface.^{33–35} Therefore, $D = 0.97 \pm 0.04$ indicates that the vapor/methanol is not only very well ordered but also with its CH₃ groups standing straight at the interface. This result is in direct disagreement with the conclusions on orientation of the interfacial methanol molecules from previous SFG-VS studies.^{6–10} This disagreement can only be ascertained by careful examination of the accuracy and effectiveness of the PNA method.

The PNA method allows direct measurement of the orientational angle of a molecular group at the interface with very high accuracy.^{11,33} In previous SFG-VS studies, the orientational angle of a molecular group was determined with the intensity ratio between SFG spectra intensities on two different polarization combinations.^{6,37} This intensity ratio method has been generally used by the SFG-VS community for determination of orientational angle of molecular groups.^{6,37} At the beginning, we thought the PNA method only to be an alternative method equivalent to the existing intensity ratio method. However, as we have pointed out previously, the accuracy of the intensity ratio method is intrinsically limited by the accuracy for intensity measurement, while the PNA method can be very accurate because it involves only polarization angle fitting.³³ Furthermore, for many molecular groups that only have one polarization with SFG intensity above the noise level, such as the CH₃ group at the vapor/methanol, vapor/acetone, and vapor/acetonitrile interfaces, the intensity ratio method can only give large uncertainty for the D value, while the PNA can be easily used for accurate determination of the value of the orientational parameter D .^{11,33,36} For example, with the intensity ratio method, Shen and Laubereau obtained $D < 1.8$ for the CH₃ group at the vapor/methanol interface, which left considerable room for speculating on the orientational angle and orientational distribution width,^{6,7} while with PNA we obtained $D = 0.97 \pm 0.04$.¹¹ In principle, the accuracy of the PNA method can be further improved experimentally with more accurate angle control and more careful measurement. The effectiveness and accuracy of the PNA method in SFG-VS has been further developed and tested with more complicated cases, such as vapor/acetone interface with two distinctively well oriented CH₃ groups.^{1,36} In addition to the advantages mentioned above, one of the most important advantages of PNA method for liquid mixture interface studies is that PNA method allows accurate measurement of orientational changes as the composition of interface changes, as we have demonstrated for the vapor/acetone–water mixture interface.¹

Thus, a well ordered first layer at the vapor/methanol interface, explicitly determined from the PNA measurement, is likely to induce ordered structure at least in the second layer from the interface,^{30,38} as we have demonstrated for the vapor/acetone–water mixture interface.¹ This would be fully consistent

with the picture suggested by Saykally et al. from EXAFS measurement of the vapor/methanol interface.¹⁴ Laubereau, Huang, and Allen et al. studied the vapor/methanol–water interface with SFG-VS previously, and they observed that the intensity of the CH₃-ss SFG spectra in ssp polarization combination decreases as the bulk methanol concentration increases above bulk mole fraction around 0.5.^{7,8,10} Their interpretations attributed this decrease in the change of the CH₃ orientation to larger θ or broader angular distribution at higher bulk concentration. Here the s polarization is perpendicular to the incident plane while the p polarization is in the incident plane. The three letter symbol ssp indicates the SF, visible, and the IR lights are in s, s, and p polarizations, respectively, and so on. As we have shown for the vapor/acetone–water mixture interface with PNA determination of the interfacial CH₃ group orientations,¹ the same phenomenon could be quantitatively accounted for with an antiparallel double layer formation as bulk concentration increases. Therefore, it is imperative for us to determine the CH₃ orientational changes for the vapor/methanol–water mixture interface with the PNA method at different bulk methanol concentrations before we can get into further interpretations on the interfacial structure and energetics of the vapor/methanol and vapor/methanol–water mixture interfaces.

In the following sections, we shall show that the PNA method in SFG-VS can be used to accurately measure the orientational parameter D values of the CH₃ groups at the vapor/methanol–water mixture interface at different bulk concentrations. These D values show that the CH₃ groups at the vapor/methanol–water mixture interface become better ordered as the bulk concentration increases. Therefore, the vapor/methanol–water mixture interface also has an antiparallel double layer structure, as we have shown for the vapor/acetone–water interface. Using the double layer adsorption model (DAM) and Langmuir isotherm, the adsorption free energies for the first and second layers are obtained. These adsorption free energies indicated that the second layer adsorption is a slightly negative adsorption, not as effective as the second layer adsorption of the vapor/acetone–water mixture interface. The origin and implication of these results on molecular interaction and liquid interface structure are also discussed.

2. Theoretical Background

The principles of SFG-VS and the theoretical treatment as well as the formula used in this report are described in detail in the first paper in this series.¹ Further detailed descriptions of the theory and formulation could be found in our previous reports.^{1,11,33,36}

Generally, the SFG intensity from a rotationally isotropic interface ($C_{\infty v}$ symmetry) in any particular polarization configuration can be expressed as^{33,37,39}

$$I(\omega) = \frac{8\pi^3 \omega^2 \sec^2 \beta}{c^3 n_1(\omega) n_1(\omega_1) n_1(\omega_2)} |\chi_{\text{eff}}^{(2)}|^2 I(\omega_1) I(\omega_2) \quad (1)$$

$$\chi_{\text{eff}}^{(2)} = N_s d(\langle \cos \theta \rangle - c \langle \cos^3 \theta \rangle) = N_s d r(\theta) \quad (2)$$

$$I(\omega) = A d^2 R(\theta) N_s^2 I(\omega_1) I(\omega_2) \quad (3)$$

$$R(\theta) = |r(\theta)|^2 = |\langle \cos \theta \rangle - c \langle \cos^3 \theta \rangle|^2 \quad (4)$$

Equation 1 is the general expression for the SFG-VS intensity as known in the literature. SHG is the degenerated case for SFG, so these expressions also stand for SHG with minor differences of constants.^{33,37} Equations 2, 3, and 4 are from our recent developments,^{33,39,40} ω , ω_1 , and ω_2 are the frequencies of the

SF signal, visible, and IR laser beam, respectively. $n_i(\omega_i)$ is the refractive index of bulk medium i at frequency ω_i , and $n'(\omega_i)$ is the effective refractive index of the interface layer at ω_i . β_i is the incident or reflection angle from interface normal of the i th light beams, and $I(\omega_i)$ is the intensity of the SFG signal or the input laser beams, respectively. The notations and the experimental geometry were described in detail previously.^{37,39}

In eq 2, N_s is the interfacial molecular number density. θ is the tilting angle between the molecular main (z') axis and the interface normal (z axis) in the laboratory coordinates. $r(\theta)$ is called the “orientational field functional” and $R(\theta)$ the “orientational functional”, which contain all molecular orientational information at a given SFG experimental configuration; while the dimensionless parameter c is called the “general orientational parameter”, which determines the orientational response $r(\theta)$ to the molecular orientation angle θ ; and d is the susceptibility strength factor, which is a constant in a certain experimental polarization configuration with a given molecular system. The d and c values are both functions of the related Fresnel coefficients including the refractive index of the interface and the bulk phases and the experimental geometry. Both d and c could be derived from the expressions of the $\chi_{\text{eff}}^{(2)}$ in relationship to the macroscopic susceptibility and microscopic (molecular) hyperpolarizability tensors for a particular molecular (microscopic) symmetry.^{1,33,39}

A is an experimental constant. It is clear that the SFG intensities for different experimental configurations are clearly parametrized in eq 3, and the term $d^2 R(\theta)$ and $r(\theta)$ play central roles in the quantitative polarization and orientation analysis of the SFG and SHG experiments.^{33,39}

For SFG-VS with contribution from multiple vibrational resonances, the SFG macroscopic susceptibility tensor $\chi_{ijk}^{(2)}$ can be written as³⁷

$$\chi_{ijk}^{(2)} = \chi_{\text{nr},ijk}^{(2)} + \sum_q \frac{A_{q,ijk}}{\omega_2 - \omega_q + i\Gamma_q} \quad (5)$$

$\chi_{\text{nr},ijk}^{(2)}$ arises from the nonresonant contribution, which is usually small if not for metal or semiconductor interfaces, and $A_{q,ijk}$, ω_q , and Γ_q are the oscillator strength, resonant frequency, and damping coefficient of the q th vibrational mode.

$$A_{q,ijk} = N_s \sum_{i'j'k'} \langle R_{ii'} R_{jj'} R_{kk'} \rangle a_{q,i'j'k'}^{(2)} \quad (6)$$

$$a_{q,i'j'k'}^{(2)} = -\frac{1}{2\epsilon_0 \omega_q} \frac{\partial \mu_{k'}}{\partial Q_q} \frac{\partial \alpha_{i'j'}}{\partial Q_q} \quad (7)$$

where $a_{q,i'j'k'}^{(2)}$ is the molecular hyperpolarizability strength tensor, $\mu_{k'}$ and $\alpha_{i'j'}$ are the infrared dipole and Raman tensor elements of the particular vibrational mode, respectively. $R_{\lambda\lambda'}$ is the element of the Euler rotational transformation matrix from the molecular coordination $\lambda'(a,b,c)$ to the laboratory coordination $\lambda(x,y,z)$.

It is easy to show that the SFG intensity and $A_{q,\text{eff}}$ in a particular polarization combination could be written in the following form.

$$I(\omega_{\text{IR}}) = C + B |\chi_{\text{nr},\text{eff}}^{(2)} + \chi_{\text{r},\text{eff}}^{(2)}(\omega_{\text{IR}})|^2 \quad (8)$$

$$= C + B \left| \chi_{\text{nr},\text{eff}}^{(2)} + \sum_q \frac{A_{q,\text{eff}}}{\omega_{\text{IR}} - \omega_q + i\Gamma_q} \right|^2 \quad (9)$$

$$A_{q,\text{eff}} \propto d_{q,\text{eff}} r(\theta) N_{s,\text{eff}} \quad (10)$$

in which $\chi_{\text{nr,eff}}^{(2)}$ and $\chi_{\text{r,eff}}^{(2)}$ are the nonresonant and resonant contributions to the SFG-VS susceptibility $\chi_{\text{eff}}^{(2)}$, respectively. B and C are two fitting constants. Therefore, the oscillator strength A_q should be proportional to the intensity factor $d_{q,\text{eff}}$ for the q th vibrational mode, orientational functional $r(\theta)$, and the interfacial density $N_{\text{s,eff}}$ in SFG-VS. It is important to note that the $d_{q,\text{eff}}$ and c values used to calculate the $A_{q,\text{eff}}$ values are dependent on the Fresnel factors at the interface, and these Fresnel factors will not be constant at different bulk concentrations if the two liquids under mixing have very different bulk refractive indexes. However, for methanol and water, their bulk refractive indexes are nearly the same, so it is valid that we use the same $d_{q,\text{eff}}$ and c values throughout the whole bulk concentration range.

Accurate information on $r(\theta)$ could be obtained by using the PNA method, which accurately determines $D = \langle \cos\theta \rangle / \langle \cos^3\theta \rangle$. With eq 4, it is clear that when $R(\theta) = 0$, $c_0 = D = \langle \cos\theta \rangle / \langle \cos^3\theta \rangle$. Therefore, the orientational parameter D could be accurately measured with the polarization null angle (PNA) method.^{11,33,36} In PNA, a polarization angle Ω_{null} for the SF signal should satisfy a zero (null) value of the SF intensity, i.e., $I(\omega) \propto |\sin(\Omega - \Omega_{\text{null}})|^2 = 0$, when the polarization angle for visible (Ω_1) and IR (Ω_2) are at fixed values, usually with $\Omega_1 = 0$ and $\Omega_2 = 45^\circ$ or -45° .¹¹ Using this accurately measured Ω_{null} value, a D value can be explicitly calculated with the known experimental configuration parameters.^{11,33,36}

It has to be emphasized that the effectiveness of the PNA method comes from the assumption that all the measured SFG-VS signal is from the interfacial species. This is generally valid for SFG-VS studies on the vapor/liquid interfaces in a reflection geometry.^{6,41–43} Especially for vapor/methanol interface, Shen et al. showed that $\chi_{Q,\text{yyz}} \approx 7 \times 10^{-19}$ esu for the methanol bulk and $\chi_{S,\text{yyz}} \approx 3.5 \times 10^{-16}$ esu for the interface.^{6,41} Therefore, the validity of the polarization analysis and the PNA method for vapor/methanol interface is guaranteed.

3. Experimental Section

Our picosecond SFG-VS spectrometer was from EKSPLA, and it has been described in detail previously.³⁹ Briefly, the 10 Hz and 23 picosecond SFG spectrometer laser system uses a co-propagating configuration. Some of the SFG polarization optics were rearranged from the original design by EKSPLA to improve the polarization control in the SFG experiment (see details below).¹¹ The visible wavelength is fixed at 532 nm and the full range of the IR tunability is 1000 to 4300 cm^{-1} . The incident angles are $\beta_1 = 62^\circ \pm 1^\circ$ for the visible beam and $\beta_2 = 52^\circ \pm 1^\circ$ for the IR beam. The SFG signal is collected around 60.5° (β) at the reflection geometry, within a small range (about 0.3°) which depends on the corresponding IR wavelength tuning range (from 2800 to 3000 cm^{-1} in the experiment). Each scan was with a 2 cm^{-1} increment and was averaged over 100 laser pulses per point. The energy of the visible beam is typically less than 300 microjoules and that of IR beam less than 200 microjoules. So the intensity in our experiment condition cannot damage or cause any heat effect and other photochemical reactions to the liquid samples. The spectrum intensity is normalized to the intensities of the corresponding visible and IR laser pulses.

The PNA experiments were performed at the peak of the CH_3 symmetric stretching mode in the SFG-VS spectra at each concentration. The polarization of the IR beam is kept at p polarization, and the polarization angle of the visible beam is -45° (positive sign is clockwise when facing the coming direction of the beam).¹¹

Particular attention has to be paid to accurate control of the polarizations in PNA experiment. We have found that in the SFG optical arrangements of the original design for the EKSPLA SFG spectrometer, the polarization of the visible beam is purely linear only for s or p polarizations. This optical arrangement is fine for measurement only with the ssp , ppp , sps , and pss polarization combinations. It had not been an issue because the general practice in the SFG-VS has not gone beyond these four polarization combinations until very recently,^{11,33} and the majority of the work only deals with the ssp or ppp polarization combination. However, in this EKSPLA design any polarization other than s or p for the visible beam is somewhat elliptical. This certainly gives incorrect null angle values when the visible polarization angle is set at $\Omega_1 = -45^\circ$. We have found out that simple adjustment of a few optical components for polarization control of the visible beam can correct the problem.¹¹ We have since made the due adjustment for all our experiments. Any laboratory that has been using the complete EKSPLA SFG spectrometer system is suggested to take notice if planning to perform any measurement with visible light polarization other than s and p . Comparison of the existing results with such measurements has to be cautiously taken.

All measurements were carried out at controlled room temperature ($22.0 \pm 0.5^\circ\text{C}$). The liquid methanol is GC grade from Fluka ($>99.0\%$), used without further treatment. Doubly distilled water was prepared with Millipore Simplicity 185 (18.2 M Ωcm). The liquid sample is filled in a round Teflon beaker (diameter ~ 5 cm) for SFG measurement. The whole experimental setup on the optical table was covered in a plastic housing to reduce the air flow and the evaporation.

4. Results and Discussion

4.1. SFG-VS Spectra, Orientation, and Double Layer Structure of the Vapor/Methanol–Water Mixture Interface. The SFG-VS spectra of the CH_3 group between 2800 and 3000 cm^{-1} were previously reported for the vapor/neat methanol interface in ssp , as well as ppp , sps , and pss polarization configurations,^{6,9,11} and vapor/methanol–water interface at different mole fractions.^{7,8,10} The ppp , sps , and pss SFG-VS spectra were all featureless and the signals were close to the noise level. There are three apparent peaks on the ssp spectra: around 2830 cm^{-1} (peak I from left), 2920 cm^{-1} (peak II), and 2945 cm^{-1} (peak III). These three peaks exhibit clear symmetric stretching characteristics according to the polarization selection rules,^{39,44} and they were assigned to the CH_3 -ss, CH_3 -Fermi, and CH_3 -Fermi modes, respectively.^{6–11}

The SFG-VS spectra we obtained for all of the four polarizations are in full agreement with the previously reported spectra of vapor/methanol interfaces. Therefore, we present only the ssp spectra for several typical bulk concentrations in Figure 1. It is clear that the intensity for the vapor/pure methanol interface (mole fraction = 1) is smaller than that for some of the vapor/methanol–water mixture interfaces, for example the one with mole fraction = 0.51. This phenomenon has been reported previously, and it was taken as evidence for a less ordered interface structure for the vapor/pure methanol interface.^{7,8,10} We plotted the CH_3 -ss peak intensity against the bulk methanol concentration and we got an almost perfect overlap with Figure 6 in the paper by Allen et al.¹⁰ This means that our data agree with their data quantitatively.

The d and c values for this ss mode in the four polarizations under our experimental condition are listed in Table 2, calculated from the following parameters: $n_1(\omega_{\text{vis}}) = 1.0$, $n_1(\omega_{\text{IR}}) = 1.0$, $n_1(\omega_{\text{SF}}) = 1.0$, $n_2(\omega_{\text{vis}}) = 1.33$, $n_2(\omega_{\text{IR}}) = 1.33$, $n_2(\omega_{\text{SF}}) = 1.33$,

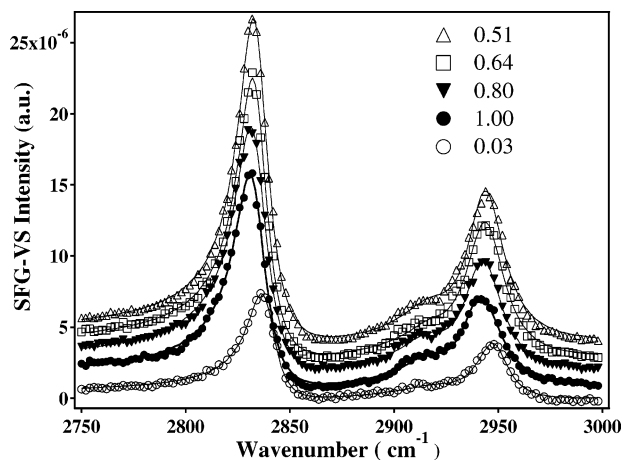


Figure 1. SFG spectra of vapor/methanol–water mixture interface at different bulk methanol mole fractions. From top to bottom are spectra for bulk mole fractions at 0.51, 0.64, 0.80, 1.00, and 0.03, respectively. The baselines of the spectra are offset for clarity. Solid lines are fitted lines with three Lorentzian peaks.

TABLE 1: Fitting Parameters for SFG-VS Spectra of CH₃-ss, Two CH₃-Fermi Peaks of Vapor/Methanol–Water Mixture Interface

mole frac	peak I (cm ⁻¹)	HWHM I (cm ⁻¹)	A _{I,eff} (a.u.)	peak II (cm ⁻¹)
0.03	2837.0 ± 0.4	8.2 ± 0.5	0.011 ± 0.001	2920.2 ± 2.6
0.10	2835.6 ± 0.2	8.4 ± 0.2	0.020 ± 0.001	2916.3 ± 2.3
0.16	2834.7 ± 0.4	8.7 ± 0.3	0.022 ± 0.001	2915.8 ± 1.8
0.23	2833.9 ± 0.3	8.8 ± 0.2	0.023 ± 0.001	2914.3 ± 1.6
0.31	2833.5 ± 0.3	8.7 ± 0.5	0.027 ± 0.001	2916.4 ± 3.8
0.40	2833.0 ± 0.1	8.6 ± 0.1	0.026 ± 0.001	2913.8 ± 3.1
0.51	2833.2 ± 0.4	8.4 ± 0.7	0.027 ± 0.001	2913.3 ± 0.9
0.64	2832.3 ± 0.6	8.4 ± 0.6	0.026 ± 0.001	2911.9 ± 2.3
0.80	2832.1 ± 0.4	8.8 ± 0.3	0.024 ± 0.001	2911.7 ± 1.2
1.00	2832.9 ± 0.7	8.6 ± 0.8	0.022 ± 0.002	2912.9 ± 3.7

HWHM II (cm ⁻¹)	A _{II,eff} (a.u.)	peak III (cm ⁻¹)	HWHM III (cm ⁻¹)	A _{III,eff} (a.u.)
12.9 ± 1.6	0.0026 ± 0.0020	2947.7 ± 0.2	9.9 ± 0.4	0.011 ± 0.001
13.2 ± 3.9	0.0040 ± 0.0007	2946.2 ± 0.3	10.6 ± 0.1	0.020 ± 0.002
14.4 ± 2.9	0.0052 ± 0.0014	2945.3 ± 0.6	11.0 ± 0.8	0.022 ± 0.002
12.4 ± 4.4	0.0042 ± 0.0013	2945.0 ± 0.5	11.3 ± 0.3	0.023 ± 0.002
14.9 ± 9.9	0.0044 ± 0.0019	2944.5 ± 0.6	12.0 ± 1.2	0.025 ± 0.003
9.6 ± 2.5	0.0030 ± 0.0008	2944.8 ± 0.3	13.0 ± 1.2	0.026 ± 0.002
9.5 ± 0.9	0.0032 ± 0.0007	2944.0 ± 0.1	13.2 ± 0.2	0.027 ± 0.002
8.4 ± 3.8	0.0022 ± 0.0011	2943.8 ± 0.5	14.3 ± 1.3	0.026 ± 0.002
8.6 ± 3.9	0.0022 ± 0.0008	2943.6 ± 0.3	14.7 ± 0.9	0.023 ± 0.002
9.3 ± 7.4	0.0014 ± 0.0010	2945.8 ± 1.5	16.8 ± 4.4	0.020 ± 0.005

TABLE 2: Values of *c* and *d* for the CH₃-ss Mode of Vapor/Methanol–Water Mixture Interface in Different Polarization Configurations

polarization	<i>c</i>	<i>d</i>
ssp	−0.259	0.342 β _{ccc} ⁽²⁾
ppp	1.318	0.163 β _{ccc} ⁽²⁾
sps	1	−0.102 β _{ccc} ⁽²⁾
pss	1	−0.100 β _{ccc} ⁽²⁾

$n'(\omega_{\text{vis}}) = 1.15$, $n'(\omega_{\text{IR}}) = 1.15$, $n'(\omega_{\text{SF}}) = 1.15$, and hyperpolarizability tensor ratio $R = \beta_{\text{aac}}^{(2)}/\beta_{\text{ccc}}^{(2)} = 1.7$.^{6,7,11,45,46} As we have pointed out, the calculated values and polarization dependence are generally not sensitive to the $n_2(\omega_{\text{IR}})$ value in a broad range for the co-propagation geometry, as we have shown before.^{37,39} Therefore, we let $n_2(\omega_{\text{IR}}) = n_2(\omega_{\text{vis}})$ in all calculations. Since the refractive index of water at room temperature is $n_{\text{water}} = 1.333$, therefore, the refractive indexes of the methanol/water mixture for different methanol concentra-

tions are nearly the same. So in all the calculations we will use the same refractive index values listed above.

As we have point out previously, a particularly important issue in quantitative polarization and orientational analysis is what is the value for the effective dielectric constant, i.e., microscopic local field factors, in the interface layer.^{11,33,37,39} A general treatment on the microscopic local field factors in a polarizable two-dimensional molecular layer was formulated by Ye and Shen in 1983.⁴⁷ Recently, a formulation for the simple liquid interface based on a modified Lorentz model was also described by Shen et al.³⁷ These two treatments agree well for simple liquid interfaces under the nonresonant conditions because the value of the linear molecular polarizability is usually small. For the sake of consistency, we shall follow the modified Lorentz model in the SFG-VS treatment of the liquid interfaces, which has been successfully applied to SFG-VS so far.^{11,37,39}

From the $d^2R(\theta)$ values, the CH₃ stretching vibration SFG intensity on ssp spectra is about 70 times stronger than those of the ppp if the orientational angle $\theta = 0^\circ$. This explains why there are no observable ppp spectra above the noise level. Accordingly, at $\theta = 0^\circ$, the sps and pss CH₃ stretching spectral intensities are essentially zero.

Fitting these SFG-VS ssp spectra with eq 9 we obtained the peak positions, widths, and oscillator strength factors ($A_{q,\text{ssp}}$) for the three vibrational bands. The results are listed in Table 1. It is interesting to note that $A_{\text{I,ssp}}$ and $A_{\text{III,ssp}}$ values are very close to each other even though the peak intensities for peak I are apparently larger than peak III. This can be understood because the spectral HMFV of peak III is broader than that of peak I. The fitted peak positions are at slightly higher wavenumbers from the apparent peak position. Both of these observations are consistent with the previously reported results and fittings.¹⁰ We also observed that all three vibrational bands red-shifted for about 5, 8, and 4 cm⁻¹, respectively, as the bulk methanol concentration increases. A similar amount of red shift was also reported by Allen et al. for the vapor/methanol–water mixture interface,¹⁰ and the same phenomenon also existed in our SFG-VS studies on the vapor/acetone–water mixture interface.¹ Because the second and the third peaks overlap each other, it is clear that there might be larger fitting errors for these two peaks, especially for peak II, which is several times weaker than peak III. Even though all our data agree quantitatively with those by Allen et al., there is one pronounced difference. All our peak positions had a 4 to 6 cm⁻¹ red-shift from those reported by Allen et al. This could be attributed to the systematic difference in wavelength calibration in different experimental systems, and this does not affect either ours or Allen's analysis of the data. However, we do find that our peak values are more close to other previously reported SFG-VS peak positions for the vapor/methanol and vapor/methanol–water mixture interfaces.^{6–9}

The null angle $\Omega_{\text{SF}}^{\text{null}}$ values at the CH₃-ss peak position for different bulk mixture concentrations are measured and listed in Table 3. The $\Omega_{\text{SF}}^{\text{null}}$ changed from $-6.7^\circ \pm 1.5^\circ$ to $-8.8^\circ \pm 1.5^\circ$ from 0.03 to 1.00 mole fraction. This is really a small change, comparing to the changes of the $\Omega_{\text{SF}}^{\text{null}}$ from $-9.7^\circ \pm 1.5^\circ$ to $-16.5^\circ \pm 1.5^\circ$ for the vapor/acetone–water mixture interface with mole fraction of 0.03 to 1.00. Such a small $\Omega_{\text{SF}}^{\text{null}}$ change comparing with the 1.5° measurement error bar indicates that the orientation of CH₃ groups of the methanol molecule at the interface might have changed, but could only have changed very little with bulk methanol concentration. The *D* values at each concentration are calculated with the relationship in eq 11,^{11,33,36} and the calculated orientational angles are listed in

TABLE 3: Measured Null Angle, Calculated Orientational Parameters, Orientational Angles, Interfacial Orientational Functional, Effective CH₃ Group Density, and Surface Coverage for the First and the Second Gibbs Adsorption Interfacial Layers at Vapor/Methanol–Water Mixture Interfaces

mole frac	$\Omega_{\text{SF}}^{\text{null}}$ (deg)	D	θ	$d_{\text{I,eff}} r(\theta)$	$N_{\text{s,eff}}^{\text{I}}$ (a.u)	$N_{\text{s,eff}}^{\text{III}}$ (a.u)	Θ	σ
0.00					0.0000	0.0000	0.00	0.00
0.03	-6.7 ± 1.5	1.01 ± 0.06	6 ± 9	1.25	0.009	0.009	0.33	0.01
0.10	-7.3 ± 1.5	0.99 ± 0.06	0 ± 12	1.26	0.016	0.016	0.64	0.03
0.16	-7.4 ± 1.5	0.98 ± 0.06	0 ± 11	1.26	0.017	0.017	0.75	0.07
0.23	-7.5 ± 1.5	0.98 ± 0.06	0 ± 11	1.26	0.018	0.018	0.83	0.11
0.31	-7.9 ± 1.5	0.96 ± 0.06	0 ± 8	1.26	0.021	0.020	0.88	0.16
0.40	-8.8 ± 1.5	0.93 ± 0.06	0 ± 0	1.26	0.020	0.021	0.91	0.23
0.51	-9.4 ± 1.5	0.91 ± 0.06	0 ± 0	1.26	0.021	0.022	0.94	0.32
0.64	-8.9 ± 1.5	0.93 ± 0.06	0 ± 0	1.26	0.020	0.021	0.97	0.46
0.80	-8.7 ± 1.5	0.94 ± 0.06	0 ± 0	1.26	0.018	0.018	0.99	0.66
1.00	-8.8 ± 1.5	0.93 ± 0.06	0 ± 0	1.26	0.017	0.016	1.00	1.00

Table 3. It is clear that throughout the whole bulk methanol concentration range, the vapor/methanol–water mixture interface is very well ordered.

$$D = \frac{\langle \cos \theta \rangle}{\langle \cos^3 \theta \rangle} = \frac{0.163 \times 1.318 + 0.342 \times 0.259 \tan \Omega_{\text{SF}}^{\text{null}}}{0.163 - 0.342 \tan \Omega_{\text{SF}}^{\text{null}}} \quad (11)$$

It is easy to find from eq 11 that if $D = \infty$, i.e., $\theta = 90^\circ$, then $\Omega_{\text{SF}}^{\text{null}} = \arctan(0.163/0.342) = 25.5^\circ$; and when $\Omega_{\text{SF}}^{\text{null}} = 0^\circ$, then $D = 1.318$, i.e., $\theta = 29.4^\circ$, assuming a δ angular distribution. These facts indicate that $\Omega_{\text{SF}}^{\text{null}}$ can indeed have enough range to provide accurate measurement on D values, and the measured $\Omega_{\text{SF}}^{\text{null}}$ values clearly indicated that the interfacial CH₃ groups oriented with very small angles from $\theta = 0^\circ$. Otherwise, the $\Omega_{\text{SF}}^{\text{null}}$ would have assumed some values more close to $\Omega_{\text{SF}}^{\text{null}} = 0^\circ$ toward the direction $\Omega_{\text{SF}}^{\text{null}} = 25.5^\circ$.

Equation 11 has slightly different coefficients from what we reported previously,¹¹ because we used a slightly different $n'(\omega_i)$ value this time. The arithmetic average of the two bulk refractive indexes, i.e., 1.16, was used for $n'(\omega_i)$ in a previous report.¹¹ We now use the modified Lorentz model estimation proposed by Shen et al.,³⁷ which gives $n'(\omega_i) = 1.15$. This difference caused a 0.04 downshift of the calculated D values, and the D values for some of the concentrations are slightly smaller than 1, as listed in Table 3. Even though the true $n'(\omega_i)$ values cannot be exactly known, and Shen et al. proposed to use $n'(\omega_i) = 1.18$ for SFG calculations for the 8CB molecular monolayer at the vapor/water interface,³⁷ none of these can change the fact that the vapor/methanol–water mixture interface is well ordered throughout the whole range of bulk methanol concentration. The trend of the measured null angle listed in Table 3 clearly shows a very small decrease, and the factor $dr(\theta)$ changed very little as the bulk methanol concentration changes throughout the whole concentration range. Therefore, we choose to stay with the value $n'(\omega_i) = 1.15$ from the modified Lorentz model in this report.³⁷

Since all the D values calculated are very close to 1, we conclude that the vapor/methanol–water mixture interface is very ordered, with the CH₃ group pointing straight up from the interface and with very narrow orientational distribution. From the trend of the $\Omega_{\text{SF}}^{\text{null}}$, we can conclude that at very low bulk methanol concentrations, the CH₃ groups at the interface may have slightly larger orientational distribution width; while at higher concentrations, the CH₃ groups are more ordered. These results do not support the interpretations of the orientational order at the vapor/methanol and vapor/methanol–water mixture interfaces from previous SFG-VS studies.^{6–10} With the facts that the interface becomes more ordered and the SFG intensity drops at higher bulk methanol concentrations, we conclude that

there is an antiparallel double layer structure at the vapor/methanol and vapor/methanol–water mixture interfaces, as discussed in detail for the vapor/acetone–water mixture interface elsewhere.¹ This picture unambiguously supports the antiparallel double layer interpretation made by Saykally et al. on the vapor/methanol interface from their EXAFS measurement.¹⁴

Following the treatment for the vapor/acetone–water mixture interface elsewhere,¹ an effective CH₃ interfacial density, $N_{\text{s,eff}}$, could be calculated from eq 10, with $N_{\text{s,eff}} = A_{\text{eff}}/(d_{\text{eff}}r(\theta))$. Here we use $A_{\text{I,eff}}$ and $A_{\text{III,eff}}$ to calculate $N_{\text{s,eff}}^{\text{I}}$ and $N_{\text{s,eff}}^{\text{III}}$, respectively. The fitting parameters for these two peaks have much better accuracy than $A_{\text{II,eff}}$, which is from the weaker peak II overlapping with peak III. The $N_{\text{s,eff}}^{\text{I}}$ and $N_{\text{s,eff}}^{\text{III}}$ values are listed in Table 3. Consequently, the double layer adsorption model (DAM), as well as the two layer Langmuir isotherms, can be applied to the $N_{\text{s,eff}}$ data. The DAM and the two-layer Langmuir isotherm are given in the following equations.¹ Detailed considerations and tests on the DAM and the different adsorption isotherms, such as Frumkin isotherm, have been discussed previously.¹

$$N_{\text{s,eff}} = N_{\text{s}}^{\text{max}}(\Theta - p\sigma) \quad (12)$$

$$\Theta = \frac{K_1 x}{1 - x + K_1 x} \quad (13)$$

$$\sigma = \frac{K_2 x \Theta}{1 - x + K_2 x} \quad (14)$$

$$N_{\text{s,eff}} = N_{\text{s}}^{\text{max}} \frac{K_1 x}{1 - x + K_1 x} \left(1 - \frac{p K_2 x}{1 - x + K_2 x} \right) \quad (15)$$

in which Θ is the first layer coverage and σ the second layer coverage, p ($-1 \leq p \leq 1$) is a proportional constant representing the efficiency for the second layer cancellation ($0 \leq p \leq 1$) or enhancement ($-1 \leq p \leq 0$), x is the bulk methanol mole fraction, and $N_{\text{s}}^{\text{max}}$ is the effective interfacial density for a full first layer coverage. K_1 and K_2 are the equilibrium constants for the first and second adsorption layer adsorptions, respectively.

Equation 15 gives a good fit for both $N_{\text{s,eff}}^{\text{I}}$ and $N_{\text{s,eff}}^{\text{III}}$ vs methanol bulk mole fraction x , as shown by the solid line in Figure 2. Through the K_1 and K_2 values the adsorption free energy for the first and second layers could be obtained according to $\Delta G_{\text{ads},i}^\circ = -RT \ln K_i$. The results are listed in Table 4. From the K_1 and K_2 values, Θ and σ at different bulk methanol concentrations are also calculated and listed in Table 3.

Thus, the first and second layer adsorption energies are $\Delta G_{\text{ads},1}^\circ = -1.6 \pm 0.1$ kcal/mol and $\Delta G_{\text{ads},2}^\circ = 0.4_{-0.3}^{+0.5}$ kcal/

TABLE 4: Fitting Results of Figure 2 with Eq 15^a

peak	N_s^{\max} (a.u.)	p	K_1	$\Delta G_{\text{ads},1}^\circ$	K_2	$\Delta G_{\text{ads},2}^\circ$
I	0.024 ± 0.002	0.30 ± 0.06	16 ± 3	-1.6 ± 0.1	0.5 ± 0.3	$0.4^{+0.5}_{-0.3}$
III	0.023 ± 0.001	0.32 ± 0.04	19 ± 3	-1.7 ± 0.1	0.32 ± 0.04	0.67 ± 0.08
average		0.31 ± 0.06	18 ± 3	-1.7 ± 0.1	0.4 ± 0.2	0.5 ± 0.4

^a The unit for $\Delta G_{\text{ads},1}^\circ$ and $\Delta G_{\text{ads},2}^\circ$ is kcal/mol.

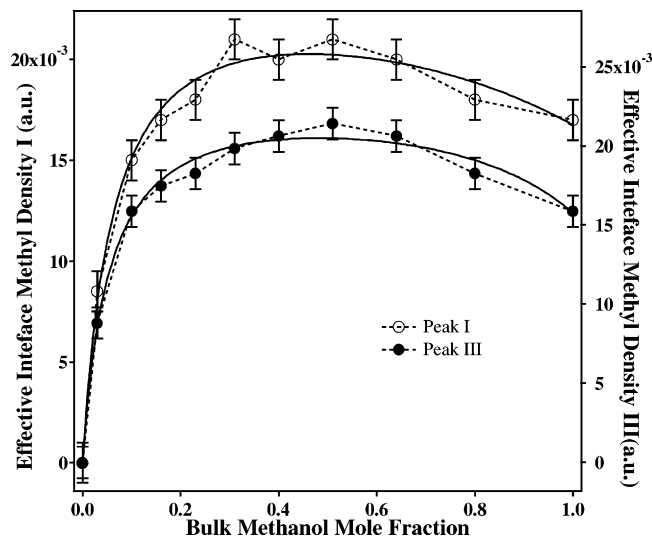


Figure 2. $N_{s,\text{eff}}^{\text{I}}$ (left: \circ) and $N_{s,\text{eff}}^{\text{III}}$ (right: \bullet) as function of the bulk methanol mole fraction. The solid lines are fittings with eq 15, while the dashed lines are the connection between neighboring points, respectively.

mol from peak I data, and $\Delta G_{\text{ads},1}^\circ = -1.7 \pm 0.1$ kcal/mol and $\Delta G_{\text{ads},2}^\circ = 0.67 \pm 0.08$ kcal/mol from peak III data, respectively. On average we have $\Delta G_{\text{ads},1}^\circ = -1.7 \pm 0.1$ kcal/mol and $\Delta G_{\text{ads},2}^\circ = 0.5 \pm 0.4$ kcal/mol, respectively.

From the surface tension data for the methanol–water mixture in the major handbooks,^{48,49} we can calculate the adsorption free energy for methanol at 20 °C. The three values we obtained are -2.1 ± 0.1 kcal/mol, -1.7 ± 0.1 kcal/mol, and -1.6 ± 0.1 kcal/mol. It is to be noted that Traube's original value listed in Langmuir's classical paper for methanol is -1.24 kcal/mol.⁵⁰ Nevertheless, these values are very close to the $\Delta G_{\text{ads},1}^\circ$ value obtained here from the SFG-VS data. It certainly confirms again the dominant contribution to the surface tension from the first adsorption layer for small polar liquid interfaces as pointed out in Langmuir's classical paper,⁵⁰ even though there is a second layer adsorption at the interface.

It is interesting to see $p = 0.31 \pm 0.06$, which is much smaller than that for vapor/acetone–water mixture interface.¹ $\Delta G_{\text{ads},2}^\circ$ for methanol aqueous solution interface is slightly positive, which indicates that the second methanol layer is more difficult to form than for the acetone aqueous solution interface, and the second layer of methanol molecules should be more likely to be thermalized since the thermal energy $kT = 0.59$ kcal/mol at room temperature. As shown in Figure 3, the second layer adsorption exhibits a slightly negative adsorption, in contrast to the positive second layer adsorption of the acetone aqueous solution interface in Figure 4.¹ There is still a possibility that the uncertainty of the fitting parameters might make the $\Delta G_{\text{ads},2}^\circ$ for methanol aqueous solution interface slightly negative, i.e., to have slightly positive second layer adsorption. However, comparison of the SFG-VS intensity behavior versus bulk methanol or acetone bulk solution showed that the vapor/acetone–water interface is with earlier intensity drop (0.2 vs 0.5 mole fraction), and more intensity drop (60% vs 40%) than

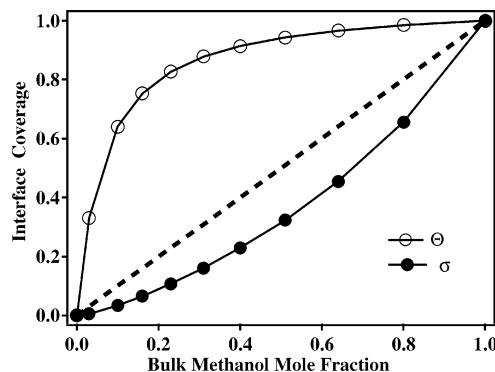


Figure 3. Interfacial coverage for the first and second layers at the vapor/methanol–water mixture interface. The dashed line is for $\Delta G_{\text{ads}}^\circ = 0$. The second layer adsorption is slightly negative adsorption.

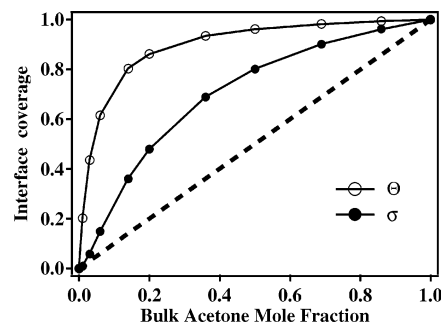


Figure 4. Interfacial coverage for the first and second layers at the vapor/acetone–water mixture interface. The dashed line is for $\Delta G_{\text{ads}}^\circ = 0$. The second layer adsorption is positive adsorption.

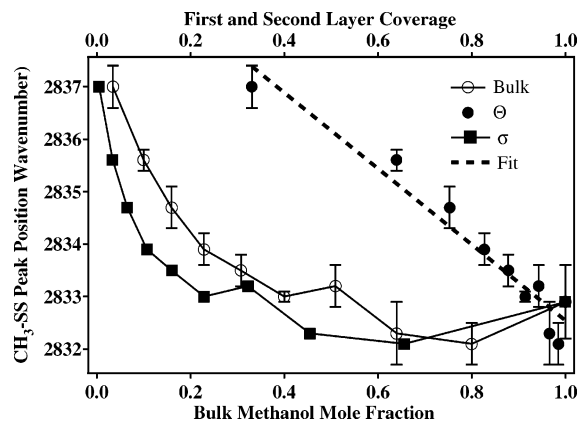


Figure 5. $\text{CH}_3\text{-SS}$ peak position as a function of bulk methanol mole fraction, first and second layer coverage. The dashed line is a linear fit. The solid lines are connection between neighboring points.

those for the vapor/methanol–water interface.¹ Therefore, the vapor/acetone–water mixture interface certainly has a stronger second layer adsorption, i.e., a more negative $\Delta G_{\text{ads},2}^\circ$ value, than that of the vapor/methanol–water mixture interface.

Structural information in the adsorbed layers can also be inferred from the SFG-VS spectral peak shift as shown in Figure 5, where the spectral shift is plotted against the bulk methanol mole fraction, first layer coverage Θ , and the second layer

coverage σ , respectively. There is a clear linear relationship between the spectral red-shift with Θ , but no such relationship between the shift and the bulk mole fraction or σ . Since the vapor/acetone–water mixture interface also showed similar red-shift dependence, it is not likely to attribute such red-shift to the changing hydrogen-bonding configurations with increasing methanol concentration.¹⁰ This first layer coverage dependence of the spectral red-shift may point to interface segregation with clusters or island structures, just as in the methanol and ethanol aqueous mixtures.^{1,3} Further investigation on this problem is certainly needed.

4.2. Structure and Energetics of the Gibbs Adsorption Layer at the Vapor/Liquid Interface.

4.2.1. The Well-Ordered Liquid Interface. SFG-VS is very powerful technique for discerning the chemistry, including structural, energetic and dynamics information, of the liquid interface. As Miranda and Shen pointed out, “SFG is currently the only technique that can yield a vibrational spectrum for a neat liquid interface”.³¹ With the interfacial vibrational spectra, the chemical species present at the interface could be identified. SFG-VS is the ideal technique for such purposes since it is a coherent polarization spectroscopy with interface selectivity and sensitivity. The capability for effective applications of SFG-VS lies at least on how well we could use the quantitative polarization analysis to solve the problems of accurate vibrational spectral assignment and of accurate determination of the interfacial molecular groups.

Shen and Hirose et al. have laid out the basis for such polarization and spectral analysis.^{37,51,52} Based on their pioneer works and using normal alcohols and diols with different chain length as examples,^{39,44} we recently demonstrated that a set of polarization selection rules for different molecular symmetry groups at the liquid interface can be developed for accurate SFG spectral assignment. This development can allow detailed analysis of the complex SFG vibrational spectra for complicated interfacial species. We have also demonstrated in this series of reports using the vapor/acetone–water mixture^{1,36} and vapor/methanol–water mixture interfaces as two unique model systems how the polarization null angle (PNA) method^{11,33,36} can help accurately determine orientational structure, adsorption structure, and energetics of these interfaces. Therefore, we can now add to Miranda and Shen and remark that SFG-VS is also currently the only technique that can yield rich spectroscopic information, and can yield detailed structural, conformational, and energetic understanding of the liquid interfaces, as well as other molecular interfaces.

Based on these developments, detailed structural and energetic information has been obtained for the vapor/acetone–water mixture and vapor/methanol–water mixture interfaces. This detailed understanding contains quite important implications on the nature of the Gibbs surface adsorption layers, and on the detailed molecular interactions at the liquid interfaces.

The liquid interface must have some neat order. Otherwise, no SFG-VS spectrum should be obtained from liquid interfaces.³¹ Molecular simulations also have shown the same story. The asymmetrical forces a molecule experiences at the liquid interface should make the interfacial molecule being oriented. Nevertheless, we are still very surprised to find out with our SFG-VS measurement and analysis that the liquid acetone and methanol interfaces are both very well ordered with very narrow orientational distributions. MD simulation has only been able to predict much broader orientational distributions for vapor/methanol–water mixture interface so far.^{17–20,22,23,25–27,29} It seems that we have to look further into the problem of molecular

orientation at the liquid interfaces, to have more quantitative understandings of the problem.

Our experimental results demonstrate that the methanol molecule has its CH_3 group point almost straight up at the vapor/methanol–water interface as well as the vapor/pure methanol interface. This seems to indicate that the hydrophobic CH_3 group of the methanol molecule tries to stay away from the hydrophilic bulk phase as far as possible. With this configuration, the O–H group of the interfacial methanol molecule points into the bulk phase, and the direction of the permanent dipole, which nearly bisects the C–O–H angle, has to point down and is 54° (or 126°) from the interface normal. This configuration should satisfy both the interfacial hydrogen bonding and the hydrophobic effect and also minimize dipole repulsion.

We have seen such subtle interplay and detailed balance of the interactions with hydrogen bonding, dipole, and hydrophobic effects for the vapor/acetone–water mixture interface.^{1,36} There are two CH_3 groups for each acetone molecule, and our SFG-VS measurement found that at the interface one of the CH_3 groups pointed away from the bulk phase, and the other pointed into the bulk phase, possibly for minimization of the dipolar repulsion between the C=O groups of the ordered interfacial acetone molecules and maximizing the hydrogen bond interaction between the water and one of the CH_3 groups of the interfacial acetone molecule. The antiparallel double layer structure should also help further minimize the dipole repulsion.

A. W. Adamson pointed out in his classical textbook *Physical Chemistry of the Interface* that “the molecule at an interface should be oriented so as to provide the most gradual possible transition from the one phase to the other”, and that “molecules will be oriented so that their mutual interaction energy will be a maximum.”^{53–56} We believe that the detailed structural information of the acetone and methanol liquid interfaces obtained from SFG-VS measurement illustrated the exactitude of these insights. We have known that the vapor/liquid interface can be used as model for the liquid/liquid interface. Experiments and theoretical simulations have repeatedly shown that the liquid/liquid interface can also be sharp and ordered to some extent.⁵⁷ Some experimental evidence suggested that diffusive liquid/liquid interfaces can exist,⁵⁸ in disagreement with predictions from MD simulation results.⁵⁹ However, the molecular structure of liquid/liquid interfaces has not yet been determined in the same molecular detail as that of the methanol and acetone interfaces. From what we have learned about the vapor/liquid interface and the experimental techniques and analysis methodology we have developed, it is highly possible that soon SFG-VS experiments can accurately reveal the detailed structure and energetics of the liquid/liquid interfaces, and we expect to see highly ordered structures similar to the vapor/liquid interfaces, even for the liquid/liquid interfaces thought to be otherwise from previously reported qualitative evidence.

4.2.2. Questions About the Antiparallel Double Layer Structure. The existence of the antiparallel double layer structure at the pure liquid methanol interface was inferred from EXAFS measurement on liquid methanol jet recently by Saykally et al.^{14,60} This structure was not supported by previous SFG-VS studies on the same interface, which inferred a more or less disordered vapor/methanol interface structure.^{6–10} Our SFG-VS measurement not only reproduced the previously reported SFG-VS data but also provided direct and accurate measurement of the interfacial CH_3 group orientation with the newly developed PNA method in SFG-VS. The PNA measurements provided the ability to separate the orientational and interfacial density contributions to the measured SFG-VS signal, so that

we have reached interpretations for an well-ordered antiparallel double layer interface structure, completely different from those in the previous SFG-VS studies on the liquid methanol interfaces. Our new interpretation provided explicit support to the antiparallel double layer interface structure proposed by Saykally et al. Similar to the vapor/acetone–water mixture interface,^{1,32} the vapor/methanol–water mixture interface also possesses an antiparallel double layer interface structure. With the same analysis, from the SFG-VS and PNA data obtained in our laboratory, along with the existing data reported previously,^{61,62} we also concluded that both the vapor/acetonitrile–water mixture interface and vapor/ethanol–water mixture interface have the same antiparallel double layer structure. Our SFG-VS and PNA data on the vapor/*tert*-butyl alcohol–water mixture interface also show an antiparallel double layer structure. These results shall be reported elsewhere soon.

Support for this antiparallel double layer structure formation also came recently. Tyrode et al. inferred an antiparallel double layer structure at the vapor/acetic acid–water mixture interface at 4 °C with polarization analysis using the polarization ratio method from their SFG-VS measurement.⁶³ The common characteristic for all the interfaces showing antiparallel double layer structure is that the SFG intensity drops at higher solute bulk concentrations in their aqueous solution. Since their data clearly showed such characteristics as above-mentioned interface systems, we believe that with the help of PNA measurement, one should be able to unambiguously confirm this antiparallel double layer structure and also obtain much more quantitative information for this very interesting interface.

Three questions naturally arises for this antiparallel double layer structure at the liquid interfaces. (1) Do all liquid interfaces forms such antiparallel double layer structure? (2) If the answer for the first question is no, what are the factors controlling whether to form such an antiparallel double layer structure? (3) What are the functions or roles of this antiparallel double layer structure at the liquid interface?

The answer for the first question is unambiguously *No*. The air/water interface has the interfacial water dipole moment nearly parallel to the interface.^{64,65} Since each water molecule underneath tends to have tetrahedral hydrogen bond structure, an antiparallel double layer structure for the air/water interface should be geometrically impossible.¹ Richmond et al. reported SFG-VS spectra of the vapor/DMSO–water mixture interface in the ssp polarization configuration.^{66,67} We reproduced their SFG-VS intensity vs bulk DMSO concentration data and confirmed that theirs is a continuous rise of the SFG intensity with increasing bulk DMSO concentration. Along with the PNA measurement data on the DMSO interface, we concluded that the vapor/DMSO–water mixture interface does not form antiparallel double layer structure. We certainly believe that there should be other liquid interfaces bearing the same characteristics as these two interfaces.

The answer to the second question could be more complicated. We surmise that one of the important clues lies in the different second layer adsorption behaviors between the vapor/acetone–water mixture interface and the vapor/methanol–water mixture interface. The first layer adsorption energies for these two interfaces are similar, being -1.9 ± 0.2 kcal/mol and -1.7 ± 0.1 kcal/mol, respectively. However, their second layer adsorption energies differ quite significantly, being -0.9 ± 0.2 kcal/mol and 0.5 ± 0.4 kcal/mol, respectively. We surmise that the first layer adsorption energy should depend on the ability of the solute molecules to replace the water molecules from the vapor/water interface, and thus to decrease the surface

TABLE 5: Pair Interaction Energies for Water, Acetone, Methanol, and DMSO Molecules^a

pair	acetone ⁷⁰	methanol ⁷⁰	methanol ⁷¹	DMSO ⁷²
AA	−5.95	−5.43	−4.46	−4.30
BB	−5.21	−4.58	−4.85	−9.94
AB	−2.53	−4.46	−4.33	−8.96
ΔW	−6.10	−1.09	−0.65	+3.68

^a The unit is kcal/mol.

tension, while the second layer adsorption should depend on the ability of the solute molecules to replace the water molecule bonded with the well ordered first layer of the solute molecule. Therefore, it is proper to further surmise that the first layer adsorption energy is a relative measurement of the hydrophobicity of a molecule, i.e., the tendency for the solute molecule to leave the bulk aqueous phase; while the second layer adsorption free energy is a relative measurement of how strong a solute molecule associates with itself. In light of this argument, we try to look into the quantities used to characterize molecular association and dispersion abilities, to understand the ability for double layer formation. In general, a Work of Association or Work of Adhesion ΔW has been defined,^{68,69}

$$\Delta W = W_{AA} + W_{BB} - 2W_{AB} \quad (16)$$

where W_{AA} , W_{BB} , and W_{AB} are the pairwise interaction energies for water–water, solute–solute, and water–solute molecules, respectively. The more negative the ΔW value, the bigger the tendency for the solute molecule to associate with itself.⁶⁸

Table 5 lists some of the pairwise interaction energies calculated using various quantum mechanical methods in the literature.^{70–72} Even though these energies may not be very accurate, and each calculation may have its own systematic errors depending on the calculation method used, comparison of the methanol value from two different sources gave quite consistent values for ΔW . Therefore, the trend of ΔW exhibited in Table 5 is nevertheless persuasive. The ΔW values indicate that in aqueous solution, acetone has the strongest tendency to associate with itself, methanol has much smaller tendency to associated with itself than acetone, and DMSO is quite unlikely to associate with itself comparing to acetone and methanol. Therefore, these ΔW values correlate very well with our observations on the relative tendency of the second layer formation for these three molecules. ΔW may be used as a measure for the ability to form the second adsorption layer, if fairly accurate pair interactions could be obtained either empirically or through theoretical computations.

The relative self-association abilities of acetone, methanol, and DMSO in their aqueous solutions may also be correlated to the relative solubility or the ability to form clusters or aggregations of these solute molecules in their aqueous solutions. It is generally known that acetone, methanol, and DMSO are liquids completely miscible with water at room temperature. Because of this simple fact, their solubility cannot be further quantified, and no quantitative solubility data for these three liquids in water can be found in the major solubility database.⁷³ Cluster and aggregation structures were reported for methanol as well as ethanol aqueous solutions previously.³ Studying the detailed self-association ability of these molecules may be an important issue, and here we propose that ΔW may become a parameter for quantification of this problem.

Above discussions also help us to understand the fact that the second layer adsorption of the vapor/methanol–water mixture interface is slightly negative. This negative adsorption means it is slightly energetically unfavorable for a methanol

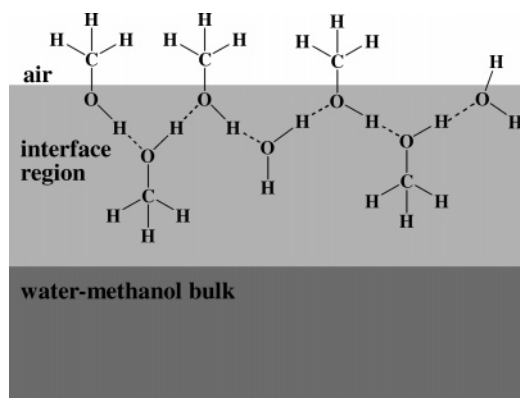


Figure 6. Schematic illustration of the possible structures for the vapor/methanol–water mixture interface. Since the hydrogen bond structure in the second layer is very similar to water or methanol molecules, it is likely that the first layer methanol molecule does not change its orientation with bulk concentration. The dotted lines represent possible hydrogen bonds.

molecule to replace a water molecule in the second layer. For the vapor/pure methanol interface there is no water molecule, and the second layer has to be occupied by methanol molecules anyway. Even though it is unfavorable to replace a water molecule with a methanol molecule in the second layer, forming the antiparallel double layer can still help reduce the total surface interaction energies.

There is a major difference between the acetone and methanol double layer structure. Acetone tends to form antiparallel dimers through nonlinear hydrogen bonding structures along with antiparallel C=O dipoles.^{32,74,75} Therefore, the building blocks for the antiparallel double layer structure at the vapor/acetone–water mixture interface are acetone dimers. However, both experiments and ab initio calculations have shown that methanol tends to form small cyclic clusters through linear hydrogen bonding structure.^{76,77} Therefore, the methanol antiparallel double layer structure tends to form double layer hydrogen network as shown in Figure 6. It is easy to see that with such an interface structure the orientation of the CH₃ group in the first adsorption layer is not likely to be affected by substitution of a water molecule in the second layer by a methanol molecule, and vice versa. This structure is well supported by our PNA SFG-VS orientation measurement. Furthermore, since each methanol molecule can donate only a single hydrogen, while each water can donate two hydrogens for hydrogen bonding, it is likely to be somewhat energetically unfavorable to replace a water molecule in the second adsorption layer with a methanol molecule. Therefore, the second layer adsorption is a negative adsorption with a slightly positive adsorption free energy.

4.2.3. New Clues on the Nature of Liquid Interface. Now we may have some clues to answer the third question about the functions and roles of the double layer structure at these liquid interfaces.

The antiparallel double layer interface structure indicates that the attractive interaction between the second layer and the third layer, if there is any, has to be relatively very weak. Therefore, the third layer and layers below are generally fully thermalized as part of the bulk solution. Structurally speaking, the thickness of the liquid interface is not more than two (antiparallel) layers. Molecular dynamics simulation has consistently obtained less than 10 Å thick density and energy profiles for the vapor/liquid and liquid/liquid interfaces, but even the best orientational profile in the interface region is not detailed enough to compare with the experimental observations here.^{59,78,79}

Such a double layer structure seems to make the interface a somewhat “detached” entity from the rest of the bulk liquid. According to the standard description in the textbook, the liquid interface is an entity with net inward forces perpendicular to it, and the interface naturally contracts.^{53,80–82} How this inward net force or inward contraction is transformed into the lateral surface tension at the interface is still without a clear microscopic interpretation. In A. W. Adamson’s classical textbook, a mechanical analogy using an axletree was offered as explanation for this problem,⁶⁹ while N. K. Adam simply stated in his classical textbook that “Surface free energy due to the inward pull on the molecules at the surface is the fundamental property of surfaces; surface tension will be taken simply as its mathematical equivalent.”⁸⁰

In light of this antiparallel double layer structure at the liquid interface, we would like to ask whether the following microscopic picture is likely. We surmise that the antiparallel double layer structure may suggest that the lateral attractive interactions between the molecules within the interfacial double layer are maximized with the preferred orientation and the inward attractive interactions from the bulk are minimized. Therefore, the tendency to contract is minimized and the interface can be more stable because of the lateral attractive forces. This interface structure is similar to the structure of the lipid double layer which generally exists in nature’s biological systems. On this basis, the term “hydrophobic packing” proposed by Saykally et al. for the vapor/pure methanol interface, did catch the essence.¹⁴

This suggestion may not be correct and further explanation has to be found for those interfaces that do not form antiparallel double layer structure. Nevertheless, the detailed liquid interface structures we have determined for the vapor/methanol–water mixture and vapor/acetone–water mixture interfaces have shed new light on these century-old fundamental problems.

5. Conclusion

In this report we studied the orientation, structure, and energetics of the vapor/methanol–water interface with SFG-VS. Different from the interpretations in previous SFG-VS studies for a more disordered interface at higher bulk methanol concentrations, we found that the methanol–water mixture interface is well ordered in the whole concentration region. We are able to do so because direct polarization null angle (PNA) measurement allowed us to accurately determine the CH₃ orientation at the interface and to separate the orientational and interfacial density contributions to the SFG-VS signal. We found that the CH₃ groups at the interface pointed out almost perpendicularly from the interface. We further found that this well-ordered vapor/methanol–water mixture interface has an antiparallel double layer structure. With the double layer adsorption model (DAM) and Langmuir isotherm, the adsorption free energies for the first and second layers are obtained as -1.7 ± 0.1 kcal/mol and 0.5 ± 0.4 kcal/mol, respectively. The second layer adsorption is slightly negative, and this means that replacement of second layer water molecule with methanol molecule is energetically unfavorable.

Comparing results from this interface with those from the vapor/acetone–water mixture interface, we are able to correlate the second layer adsorption free energy with the parameter generally used to characterize solute self-association and dispersion in solvent, using simple pairwise self- and mutual interaction energies between the water and solute molecules. Unlike the vapor/acetone–water mixture interface, whose antiparallel double layer structure consists antiparallel acetone dimers, the

vapor/methanol–water mixture interface may have an antiparallel double layer with a laterally extended hydrogen bond network. This structure explains nicely why the orientational angle CH_3 groups in the first adsorption layer do not change with the adsorption of the second methanol layer. These results provided explicit support for the “hydrophobic packing” structure inferred by Saykally et al. from their EXAFS measurement on the liquid methanol jet interface.¹⁴ These results have provided detailed microscopic structural evidence for the understanding of liquid interfaces. The techniques and methodology used in this study can be generally applied for better understanding of molecular liquid interfaces, as well as other molecular interfaces.

Note Added in Proof: Just after we finished the draft of this manuscript, Dr. Pali Jedlovsky informed us that their Monte Carlo simulation using the bivariate statistics indicated the CH_3 group of methanol standing straight at the vapor/water interface at different bulk methanol concentrations. They also found a double layer structure, the outmost layer is rich in methanol, followed by a water-rich, methanol-poor inner layer. Beyond this layer both components reach the bulk density.

Acknowledgment. H.F.W. thanks the Chinese Academy of Sciences (the Hundred Talent Program starting fund), the Natural Science Foundation of China (NSFC No. 20274055, No. 20425309), and the Chinese Ministry of Science and Technology (MOST No. G1999075305) for support. We thank Wen-kai Zhang for compilation of the pairwise interaction data from literature.

References and Notes

- (1) Chen, H.; Gan, W.; Wu, B. H.; Wu, D.; Guo, Y.; Wang, H. F. *J. Phys. Chem. B* **2005**, *109*, 8053–8063.
- (2) Franks, F.; Ives, D. J. G. *Quart. Rev.* **1962**, *20*, 1–45.
- (3) Dixit, S.; Crain, J.; Poon, W. C. K.; Finney, J. L.; Soper, A. K. *Nature* **2002**, *416*, 829–832, and references therein.
- (4) Lawrence, K. I.; Dlott, D. D. *Chem. Phys. Lett.* **2000**, *321*, 419–425.
- (5) Dlott, D. D. *Chem. Phys.* **2001**, *266*, 149–166.
- (6) Superfine, R.; Huang, J. Y.; Shen, Y. R. *Phys. Rev. Lett.* **1991**, *66*(8), 1066–1069.
- (7) Wolfrum, K.; Graener, H.; Laubereau, A. *Chem. Phys. Lett.* **1993**, *213*, 41–46.
- (8) Huang, J. Y.; Wu, M. H. *Phys. Rev. E* **1994**, *50*, 3737–3746.
- (9) Stanners, C. D.; Du, Q.; Chin, R. P.; Cremer, P.; Somorjai, G. A.; Shen, Y. R. *Chem. Phys. Lett.* **1995**, *232*, 407–413.
- (10) Ma, G.; Allen, H. C. *J. Phys. Chem. B* **2003**, *107*, 6343–6349.
- (11) (a) Lu, R.; Gan, W.; Wang, H. F. *Chin. Sci. Bull.* **2003**, *48*(20), 2183–2187. (b) Lu, R.; Gan, W.; Wang, H. F. *Chin. Sci. Bull.* **2004**, *49*(9), 899.
- (12) Van Loon, L. L.; Allen, H. C. *J. Phys. Chem. B* **2004**, *108*, 17666–17674.
- (13) Braslau, A.; Pershan, P. S.; Swislow, G.; Ocko, B. M.; Als-Nielsen, J. *Phys. Rev. A* **1988**, *38*, 2457–2470.
- (14) Wilson, K. R.; Schaller, R. D.; Co, D. T.; Saykally, R. J. *J. Chem. Phys.* **2002**, *117*, 7738–7744.
- (15) Wilson, K. R.; Rude, B. S.; Smith, J.; Cappa, C.; Co, D. T.; Schaller, R. D.; Larsson, M.; Catalano, T.; Saykally, R. J. *Rev. Sci. Instrum.* **2004**, *75*, 725–736.
- (16) Penfold, J. *Rep. Prog. Phys.* **2001**, *64*, 777–814.
- (17) Matsumoto, M.; Kataoka, Y. *J. Chem. Phys.* **1989**, *90*, 2398–2407.
- (18) Yang, B.; Sullivan, D. E.; Gray, C. G. *J. Chem. Phys.* **1991**, *95*, 7777.
- (19) Matsumoto, M.; Takaoka, Y.; Kataoka, Y. *J. Chem. Phys.* **1993**, *98*, 1464–1472.
- (20) Matsumoto, M.; Mizukuchi, H.; Kataoka, Y. *J. Chem. Phys.* **1993**, *98*, 1473–1485.
- (21) Matsumoto, M.; Yasuoka, K.; Kataoka, Y. *J. Chem. Phys.* **1994**, *101*, 7912–7917.
- (22) Benjamin, I. *Phys. Rev. Lett.* **1994**, *73*, 2083–2086.
- (23) Dietter, J.; Morgner, H. *J. Phys.: Condens. Matter* **1996**, *8*, 3767–3784.
- (24) Wilson, M. A.; Pohorille, A. *J. Phys. Chem. B* **1997**, *101*, 3130–3135.
- (25) Zakharov, V. V.; Brodskaya, E. N.; Laaksonen, A. *J. Chem. Phys.* **1998**, *109*, 9487–9493.
- (26) Dang, L. X.; Chang, T. M. *J. Chem. Phys.* **2003**, *119*, 9851–9857.
- (27) Lopez-Lemus, J.; Alejandre, J. *Mol. Phys.* **2003**, *101*, 743–751.
- (28) Taylor, R. S.; Shields, R. L. *J. Chem. Phys.* **2003**, *119*, 12569–12576.
- (29) Dang, L. X. *J. Phys. Chem. A* **2004**, *108*, 9014–9017.
- (30) Good, R. J. *J. Phys. Chem.* **1957**, *61*, 810–813.
- (31) Miranda, P.; Shen, Y. R. *J. Phys. Chem. B* **1999**, *103*, 3292–3307, and references therein.
- (32) Yeh, Y. L.; Zhang, C.; Held, H.; Mebel, A. M.; Wei, X.; Lin, S. X.; Shen, Y. R. *J. Chem. Phys.* **2001**, *114*, 1837–1843.
- (33) Rao, Y.; Tao, Y. S.; Wang, H. F. *J. Chem. Phys.* **2003**, *119*, 5226–5236.
- (34) Simpson, G. J.; Westerbuhr, S. G.; Rowlen, K. L. *Anal. Chem.* **2000**, *72*, 887–898.
- (35) Simpson, G. J.; Rowlen, K. L. *J. Am. Chem. Soc.* **1999**, *121*, 2635–2636.
- (36) Chen, H.; Gan, W.; Wu, B. H.; Zhang, Z.; Wang, H. F., submitted to *Chem. Phys. Lett.*
- (37) Zhuang, X.; Miranda, P. B.; Kim, D.; Shen, Y. R. *Phys. Rev. B* **1999**, *59*, 12632–12640.
- (38) Henniker, J. C. *Rev. Mod. Phys.* **1949**, *21*, 322–341.
- (39) Lu, R.; Gan, W.; Wu, B. H.; Chen, H.; Wang, H. F. *J. Phys. Chem. B* **2004**, *108*, 7297–7306.
- (40) Wang, H. F. *Chin. J. Chem. Phys. (English)* **2004**, *17*, 362–368.
- (41) Shen, Y. R. *Appl. Phys. B* **1999**, *68*, 295–300.
- (42) Wei, X.; Hong, S. C.; Lvovsky, A. I.; Hermann, H.; Shen, Y. R. *J. Phys. Chem. B* **2000**, *104*, 3349–3354.
- (43) Hermann, H.; Lvovsky, A. I.; Wei, X.; Shen, Y. R. *Phys. Rev. B* **2002**, *66*, 205110.
- (44) Lu, R.; Gan, W.; Wu, B. H.; Chen, H.; Wang, H. F., submitted to *J. Phys. Chem. B*.
- (45) Colles, M. J.; Griffiths, J. E. *J. Chem. Phys.* **1972**, *56*, 3384–3391.
- (46) Zhang, D.; Gutow, J.; Eisenthal, K. B. *J. Phys. Chem.* **1994**, *98*, 13729–13734.
- (47) Ye, P. X.; Shen, Y. R. *Phys. Rev. B* **1983**, *28*, 4288–4294.
- (48) *Landolt-Börnstein IV-16: Surface Tension of Pure Liquids and Binary Liquid Mixtures*; Lechner, M. D., Ed.; Springer: Berlin, 1997.
- (49) *The Physico-chemical Constants of Binary Systems in Concentrated Solutions*; Timmermans, J., Ed.; Wiley-Interscience, New York, 1960; Vol. 4.
- (50) Langmuir, I. *J. Am. Chem. Soc.* **1917**, *39*, 1848–1906.
- (51) Hirose, C.; Akamatsu, N.; Domen, K. *J. Chem. Phys.* **1992**, *96*(2), 997–1004.
- (52) Hirose, C.; Yamamoto, H.; Akamatsu, N.; Domen, K. *J. Phys. Chem.* **1993**, *97*, 10064–10069.
- (53) Adamson, A. W. *Physical Chemistry of Surfaces*, 5th ed.; Wiley-Interscience: New York, 1990; p 69.
- (54) Hardy, W. B. *Proc. R. Soc. (London)* **1913**, *A88*, 303.
- (55) Harkins, W. D. *Z. Phys. Chem.* **1928**, *139*, 647.
- (56) Harkins, W. D. *The Physical Chemistry of Surface Films*; Reinhold, New York, 1952.
- (57) *The Dynamics and Structure of the Liquid–Liquid Interface, Faraday Discussion Vol. 129*, Fitzwilliam College, Cambridge, U.K., Sep 1–3, 2004.
- (58) Walker, D. S.; Brown, M. G.; McFearn, C. L.; Richmond, G. L. *J. Phys. Chem. B* **2004**, *108*(7), 2111–2114.
- (59) Jedlovsky, P.; Vincze, A.; Horvai, G. *J. Chem. Phys.* **2002**, *117*, 2271–2280.
- (60) Rossky, P. J. *Nature* **2002**, *419*, 889–890.
- (61) Kim, J.; Chou, K. C.; Somorjai, G. A. *J. Phys. Chem. B* **2003**, *107*, 1592–1596.
- (62) Sung, J.; Park, K.; Kim, D. *J. Korean Phys. Soc.* **2004**, *44*, 1394–1398.
- (63) (a) Tyrode, E.; Johnson, C. M.; Baldelli, S.; Leygraf, C.; Rutland, M. W. *J. Phys. Chem. B* **2004**, *109*, 321–328. (b) Johnson, C. M.; Tyrode, E.; Baldelli, S.; Leygraf, C.; Rutland, M. W. *J. Phys. Chem. B* **2004**, *109*, 328–341.
- (64) Townsend, R. M.; Rice, S. A. *J. Chem. Phys.* **1991**, *94*, 2207–2218.
- (65) Du, Q.; Superfine, R.; Freysz, E.; Shen, Y. R. *Phys. Rev. Lett.* **1993**, *70*(15), 2313–2316.
- (66) Allen, H. C.; Gragson, D. E.; Richmond, G. L. *J. Phys. Chem. B* **1999**, *103*, 660–666.
- (67) Allen, H. C.; Raymond, E. A.; Richmond, G. L. *Curr. Opin. Coll. Inter. Sci.* **2000**, *5*, 74–80.
- (68) Israelachvili, J. N. *Intermolecular and Surface Forces*, 2nd ed.; Academic Press: London, 1991; Chapter 9.
- (69) Adamson, A. W.; Gast, A. P. *Physical Chemistry of Surfaces*, 6th ed.; Wiley-Interscience: New York, 1997; Chapter III.
- (70) Freitas, L. C. G.; Cordeiro, J. M. M.; Garbujo, F. L. L. *J. Mol. Liq.* **1999**, *79*, 1–15.

- (71) Huang, N.; MacKerell, A. D., Jr. *J. Phys. Chem. A* **2002**, *106*, 7820–7827.
- (72) Kirchner, B.; Hutter, J. *Chem. Phys. Lett.* **2002**, *364*, 497–502.
- (73) IUPAC–NIST Solubility Database can be searched at <http://srdata.nist.gov/solubility/>
- (74) Jedlovsky, P.; Palinkas, G. *Mol. Phys.* **1995**, *84*, 217.
- (75) Hermida-Ramón, J. M.; Ríos, M. A. *J. Phys. Chem. A* **1998**, *102*, 2594–2602.
- (76) Buck, U.; Siebers, J. G.; Wheatley, R. J. *J. Chem. Phys.* **1998**, *108*, 20–32.
- (77) Provencal, R. A.; Paul, J. B.; Roth, K.; Chapo, C.; Casaes, R. N.; Saykally, R. J.; Tschumper, G. S.; Schaefer, H. F., III. *J. Chem. Phys.* **1999**, *110*, 4258–4267.
- (78) Benjamin, I. *Chem. Rev.* **1996**, *96*, 1449–1475.
- (79) Benjamin, I. *Annu. Rev. Phys. Chem.* **1997**, *48*, 407–451.
- (80) Adam, N. K. *The Physics and Chemistry of Surfaces*, 3rd ed.; Clarendon Press: Oxford, 1941.
- (81) Davies, J. T.; Rideal, E. K. *Interfacial Phenomena*; Academic Press: New York, 1963.
- (82) Shaw, D. J. *Introduction to Colloid & Surface Chemistry*, 4th ed. Butterworth Heinemann: Oxford, 1992.